Testing Pear Disease Diagnosis Assuming Gaussian Distribution of Feature Values

Nikos Petrellis

Department of Electrical and Computer Engineering, University of Peloponnese, Patra, Greece; e-mail: npetrellis@uop.gr

Abstract. A plant disease diagnosis method based on processing images that display a sick plant part, is tested here on four pear diseases. In the original classification method employed, an extensible feature ranking method had been adopted. Specifically, a discrete grade was assigned to each invariant feature depending on whether its value was found within predefined strict or loose limits. The potential classes that may correspond to the test sample, were sorted according to the sum of the grades of the features. In the current implementation, a Gaussian behavior is assumed and an analog feature grade is assigned depending on the distance of the extracted feature value from the mean. Modeling feature values with Gaussian distribution would eliminate the need of heuristic selection of the strict/loose feature limits but would make more difficult the extension of the supported set of diseases by the end user. However, the experimental results show that the feature values do not follow a Gaussian distribution since comparable classification precision results are obtained only when a normalization scheme is applied to the input image.

Keywords: plant disease diagnosis; Gaussian distribution; normalization; image processing; smart phone application.

CEUR-WS.org/Vol-2761/HAICTA_2020_paper20.pdf

1 Introduction

Plant monitoring is important in precision agriculture and similar Internet of Things (IoT) applications [1][2]. Plant pathogen diagnostics are reviewed in [3]. A review of machine vision techniques employed for the inspection of citrus fruits with accuracy ranging between 60% and 100% is presented in [4]. Several monitoring techniques for specific plants have been recently proposed for garden strawberry diseases [5], rice blast [6], Fusarium infections on wheat [7], etc. Image processing in color scale different than Red-Green-Blue (RGB) has also been employed for plant disease diagnosis. For example, CIE L*a*b color scale is employed in [8] and a neural network achieves 91% classification accuracy. The use of hyperspectral data and neural networks in plant disease diagnosis is reviewed in [9]. Mobile phone applications for the recognition of plant diseases have also been presented in [10] (Purdue Plant Doctor implemented for iOS and Android) and [11] for Android.

Copyright © 2020 for this paper by its authors. Use permitted under Creative Commons License Attribution 4.0 International (CC BY 4.0).
Proceedings of the 9th International Conference on Information and Communication Technologies in Agriculture, Food & Environment (HAICTA 2020), Thessaloniki, Greece, September 24-27, 2020.

In this paper, an alternative implementation of the smart phone application originally presented in [12] and extended in [13] to support several color normalization techniques, is used. At the input of this smart phone application, an image is used of the plant part displaying the symptoms of a disease as a number of lesion spots. The image is segmented to the background (ignored), the normal leaf or fruit, the spots and halo around the spots. A number of invariant features concerning the 3 Regions of Interest (ROI) are used for the classification. In the previous versions, a small number of representative training images were used for each disease to arbitrarily extract strict and loose limits for each feature. During the test phase, the extracted new feature value was compared to the extracted limits defined for a specific disease and different grade was assigned according to whether the new feature value resided within the strict or loose limits. The weighted sum of all feature grades was used to sort the potential diseases that may have infected the plant. This method will be called henceforth Limit Test (LT).

The alternative classification method tested here, assumes that the values of each feature found in images displaying the same disease, follow a Gaussian Distribution (GD). During the training phase, the various values of a specific feature are used to estimate its mean and variance that are stored in the signature (recognition rules) of a specific disease. The grade assigned to each feature depends, in this case, on the distance of the current feature value from the mean. Two cases are examined: a) use of the original images without normalization and b) use of Linear Dynamic Range Expansion (LDRE normalization) for each one of the RGB colors to moderate the differences in the light exposure of each photograph. Sensitivity, specificity, precision and accuracy metrics are used to evaluate the LT and GD classification methods. The pear diseases tested with the methods described above include: Fire Blight, Pear Scab, Mycosphaerella and Powdery Mildew. Fifty photographs displaying the upper surface of a pear leaf have been tested from each disease.

The LT, GD classification methods are described in Section 2. The experimental results are presented and discussed in Section 3.

2 Plant Disease Recognition Methods

The photographs of plant parts captured by the user must display indicative lesions (spots) of a specific disease. The plant parts can be leaves or fruits or even roots, branches, flowers, etc. The user initially selects the user interface language, the image normalization type and the halo zone around the lesion spots with its thickness expressed as a number of pixels (see Fig. 1a). Then, the photograph is analyzed by potentially configuring the thresholds for the separation of the background, the normal plant part and the lesion. In the present application version, separate thresholds are used for each color component of the RGB color scale (red, green, blue) as shown in Fig. 1b. Additional information can be given by the user to assist the disease classification (e.g., weather data of the specific rural region where the plant exists, located by Global Positioning System-GPS). The smart phone application was initially developed for Windows Phone and then ported to Android platforms. The classification methods are described in detail and the reader can refer to [13] for more implementation details concerning the application.

(a) (b) (c) (d)

Fig. 1. The basic application pages. Selection of language, normalization type and halo thickness (a), photo selection and analysis (b), updated photo using LDRE normalization (c) and list of extracted features (d).

The following invariant features are extracted by the segmented photograph: number of lesion spots, their area, the average gray level of each region (normal plant part, spots, halo). A separate histogram is generated for each color component (red, green, blue) and each ROI (normal, spots, halo). It is assumed that photographs displaying the same disease would have similar features like the ones listed above. Instead of attempting to match full histograms, their similarity is simply checked by comparing where they start, where they end and the where their peak is (the histograms usually consist of a single lobe).

When the input photograph is analyzed two triplets of thresholds are used to separate the background and the spots. If all the red, green, blue values of a pixel (p_r, p_g, p_b, respectively) are higher than the corresponding background thresholds (BG_r, BG_g, BG_b) then, this pixel is mapped to the background since the background in this implementation is simply assumed to be much brighter than the plant part. The rest of the pixels are initially mapped as normal plant part (e.g., the leaf in the cases examined here). The lesion spots can either be darker or brighter (the user indicates this fact to the application through the Invert checkbox shown in Fig. 1b), than the normal leaf. If all the p_r, p_g, p_b values of a leaf pixel are lower than the corresponding thresholds TH_r, TH_g, TH_b and the lesion is darker than the normal leaf color, this pixel is mapped to the lesion region. If the p_r, p_g, p_b values of a leaf pixel are higher than the corresponding thresholds TH_r, TH_g, TH_b and the lesion is brighter than the normal leaf, again this pixel is mapped to the lesion region. Finally, the pixels existing in a zone around the spots with thickness defined by the corresponding field shown in Fig. 1a, are mapped to the halo region. The user can also select an image normalization method from the page shown in Fig. 1a. The supported normalization methods are described in detail in [13]. In this paper, the normalization Type 1 (no normalization) and Type 2 (LDRE in all RGB colors) are tested since Type 2 seems to achieve a better classification accuracy [13] compared with the other supported normalization schemes.

The matrix BGW1 is defined with the same size as the original image and each one of its cells can have four distinct values corresponding to normal leaf, spot, hallo and background. Matrix BGW2 can be derived from BGW1 by marking pixels belonging

to the same spot with the same identity. BGW2 can be used to estimate all of the features used, in a simple way. The maximum spot identity is the number of spots while the area covered by the spots is estimated by the number of spot pixels divided by the total number of pixels belonging to the plant part. The average gray level of each region can be estimated by averaging the gray level of the pixels mapped to this region in BGW2. Spots consisting of a very small number of pixels (less than the threshold "Min Area" of Fig. 1a) are considered as noise and are not taken into consideration.

During the training phase of the application for a new disease, a small number of representative photos with similar sick plant parts can be analyzed even by an end user that is not aware of the application architecture and implementation details. The range of each feature f_i as determined by the training photographs is used to define the strict limits [f_{i_s1}..f_{i_s2}]. This narrow range can be heuristically extended in order to define the loose limits [f_{i_l1}..f_{i_l2}] of this feature for a specific disease. The application lists all these limits to the end user as shown in Fig. 1d, to assist the definition of new diseases or for the customization of the existing diseases. All the feature strict and loose limits are stored in a disease signature exploited during the test phase. When a new photograph is examined in the test phase, all the features f_i are extracted and are compared to the predefined limits stored in each disease signature. A rank *Gr* is estimated for each potential disease using the following equation:

$$Gr = \sum_i x_{i\_l} w_{i\_l} + \sum_i x_{i\_s} w_{i\_s} \quad (1)$$

$$x_{i\_l} = \begin{cases} 1, if\ f_{i\_l1} \le f_i \le f_{i\_l2} \\ 0, otherwise \end{cases}. \quad (2)$$

$$x_{i\_s} = \begin{cases} 1, if\ f_{i\_s1} \le f_i \le f_{i\_s2} \\ 0, otherwise \end{cases}. \quad (3)$$

The parameters w_{i_l} and w_{i_s} are the individual grades (weights) assigned to feature f_i if it is found within the loose or strict limits, respectively of a specific disease. The diseases are sorted according to the rank *Gr* that they have received for a specific photograph. The three diseases with the highest rank are listed. The simple classification method described above is the LT.

The new classification method (GD) tested in this paper assumes that the feature values that are extracted from the photographs of a disease training set, follow a Gaussian distribution. The mean feature value $f_{m,i}$, is estimated by the training samples. The rank G_i given for this feature is inversely proportional to the distance of the value of this feature from $f_{m,i}$. If σ^2 is the variance for this feature (also estimated by the training samples), then the disease rank *Gr* can be estimated by:

$$Gr = \sum_{i=1}^{N-1} \frac{w_i}{\sqrt{2\pi\sigma^2}} e^{-\frac{(f_i - f_{m,i})^2}{2\sigma^2}}. \quad (4)$$

The LDRE normalization employed in the experiments performed in the context of this paper, stretches the values of each color component in the RGB scale according to the following equation:

$$NewCol = \frac{PrevCol - MinGray}{MaxGray - MinGray} Range + StartCol \quad (5)$$

PrevCol is the original color value, *MinGray* and *MaxGray* are the minimum and maximum pixel values of the gray version of the image (excluding the background), *Range* is the desired final range and *StartCol* is the desired offset where *Range* starts.

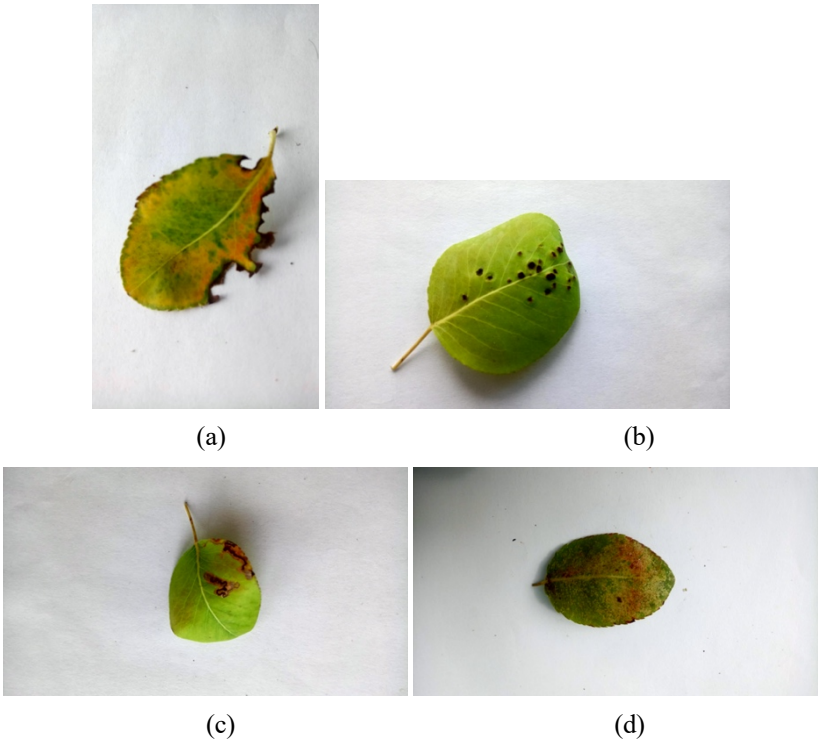

(a) (b)

(c) (d)

Fig. 2. Indicative photographs from the tested pear diseases: fire blight (a), pear scab (b), mycosphaerella leaf spot (c) and powdery mildew (d).

3 Experimental Results

Indicative photographs from the pear diseases that have been tested in the framework of this paper are shown in Fig. 2. The metrics used to compare the LT and GD classification methods are the sensitivity, specificity, precision and accuracy. Let True Positives (TP) be the number of photographs that are correctly recognized as positive to a disease. True Negatives (TN) are the number of photographs that are correctly recognized as negative to a disease. False Positives (FP) are the photographs that are falsely recognized as positives and False Negatives (FN), the ones that are falsely recognized as negatives to a disease. The aforementioned four metrics are defined as:

$$Sensitivity = \frac{TP}{TP + FN} \quad (6)$$

$$Specificity = \frac{TN}{TN + FP} \quad (7)$$

$$Precision = \frac{TP}{TP + FP} \quad (8)$$

$$Accuracy = \frac{TP + TN}{TP + TN + FP + FN} \quad (9)$$

As already mentioned, 50 photographs of each pear disease have been tested. They have been retrieved from pear trees in the Achaia prefecture of Greece. About half of these photographs have been captured under sunlight and the rest, under a canopy in order to test different light exposure. Eight representative (training) photographs have been used to extract the disease recognition signatures in either LT (containing the loose and strict limits of each feature), or GD (containing the mean and variance of each feature). In the first test case, the photographs have not been normalized. The experimental results for this case are shown in Tables 1 and 2.

Table 1. LT classification method without normalization.

Disease	Sensitivity	Specificity	Precision	Accuracy
Fire blight	0.89	0.92	0.78	0.91
Pear scab	0.44	1	1	0.86
Mycosphaerella leaf spot	1	0.85	0.69	0.89
Powdery Mildew	0.98	1	1	0.99
Average	**0.83**	**0.94**	**0.87**	**0.91**

Table 2. GD classification method without normalization.

Disease	Sensitivity	Specificity	Precision	Accuracy
Fire blight	0	0.75	0	0.57
Pear scab	0.96	0.67	0.51	0.87
Mycosphaerella leaf spot	0.88	0.99	0.96	0.96
Powdery Mildew	0.06	0.97	0.43	0.73
Average	**0.48**	**0.85**	**0.47**	**0.78**

As can be seen from the results listed in Tables 1 and 2, GD is much worse than LT since 2 of the 4 diseases (fire blight and powdery mildew) cannot be recognized at all: their sensitivity is 0 although the specificity achieved is more acceptable. Using LT as the classification method, only pear scab has a low sensitivity but all the average metrics are better than GD.

If image normalization with LDRE is used, the results obtained are listed in Tables 3 and 4. Although the average values of the 4 metrics obtained for GD are still worse than the ones achieved by LT, they are much closer with LDRE normalization. In any

case, these results show that although Gaussian seems a more natural way to describe the distribution of the various feature values, the classification accuracy achieved by GD is worse than the one achieved by LT. The positive aspect of this conclusion is that the rules in the disease signatures used by LT can be defined in a simpler way by an end-user that is not familiar with the implementation details of the developed application: it is easier for an end-user to determine the limits in a list of feature values than estimate the mean values and variances required by the GD. For this reason, the employed LT classification method allows the extension of the supported set of diseases by an end user that is not particularly qualified in computer science or statistics.

Table 3. LT classification method with LDRE normalization.

Disease	Sensitivity	Specificity	Precision	Accuracy
Fire blight	0.92	0.85	0.67	0.87
Pear scab	0.56	0.97	0.87	0.87
Mycosphaerella leaf spot	0.96	1	1	0.99
Powdery Mildew	1	0.99	0.96	0.99
Average	**0.86**	**0.95**	**0.87**	**0.93**

Table 4. GD classification method with LDRE normalization.

Disease	Sensitivity	Specificity	Precision	Accuracy
Fire blight	0.83	0.87	0.67	0.86
Pear scab	0.58	0.93	0.74	0.84
Mycosphaerella leaf spot	0.89	1.00	1.00	0.97
Powdery Mildew	0.88	0.98	0.93	0.96
Average	**0.79**	**0.95**	**0.83**	**0.91**

5 Conclusions

Two classification methods are tested in the framework of a mobile phone application capable of recognizing pear diseases. The experimental results showed that the classification method based on the assumption that the invariant image feature values follow a Gaussian distribution in images displaying the same disease, does not achieve a better accuracy than the heuristic classification method that compares if the feature values reside within predefined strict and loose limits. The benefit from the classification method based on Gaussian distribution is that it favors the extensibility of the supported set of diseases by a non-expert. Image normalization significantly improves the accuracy of this classification method.

Based on the experimental results presented in this paper, future work may focus on supporting multiple ranges of feature values for comparison e.g., too strict, strict, loose, too loose, etc, in order to improve further the accuracy.

Acknowledgments. This work is protected by the provisional patents 1009346/13-8-2018 and 1008484/12-5-2015 (Greek Patent Office). The author wishes to thank the

student Olympia Sakorafa for her contribution in the experiments carried out for this paper.

References

1. Lara, J.C.D., Gutierrez, S., Rodríguez, F. (2019) Low Cost Greenhouse Monitoring System Based on Internet of Things. Proc. Of the 2019 IEEE International Conference on Engineering Veracruz (ICEV), Mexico.
2. Nayak, P., Kavitha, K. and Rao. C.M. (2020) IoT-Enabled Agricultural System Applications, Challenges and Security Issues. IoT and Analytics for Agriculture, DOI: 10.1007/978-981-13-9177-4_7.
3. Rani, A., Donovan, N. and Mantri, N. (2019) Review: The future of plant pathogen diagnostics in a nursery production system. Elsevier Biosensors and Bioelectronics. Available online.
4. Cubero, S., Lee, W.S., Aleixos, N., Albert, F. and Blasco, J. (2016) Automated Systems Based on Machine Vision for Inspecting Citrus Fruits from the Field to Postharvest—a Review. Food and Bioprocess Technology, 9(10), p. 1623–1639.
5. Aleinikov, A.F. (2018). Method of Non-Invasive Determination of Fungal Diseases of Common Garden Strawberry. Siberian Herald of Agricultural Science, 48(3).
6. Chen, W.L., Lin, Y.B., Ng, F.L., Liu, C.Y. and Lin, Y.W. (2019) RiceTalk: Rice Blast Detection using Internet of Things and Artificial Intelligence Technologies. IEEE Internet of Things Journal
7. Bauriegel, E. and Herppich, W.B. (2014) Hyperspectral and Chlorophyll Fluorescence Imaging for Early Detection of Plant Diseases, with Special Reference to Fusarium spec. Infections on Wheat. Agriculture, 4, p. 32-57.
8. Kulkarni A. and Patil, A. (2012) Applying Image Processing Technique to Detect Plant Diseases. International Journal of Modern Engineering Research, 2(5), p. 3361-3364.
9. Siva, K.G., Ganesan, B. and Pradhan, V.B. (2018). A Review of Neural Networks in Plant Disease Detection using Hyperspectral Data. Elsevier Information Processing in Agriculture, 5(3), p. 354-371
10. Luke, E., Beckerman, J., Sadof, C., Richmond, D., McClure, D., Hill,M. and Lu, Y. (2017) Purdue Plant Doctor App Suite. Purdue University, https://www.purdueplantdoctor.com/. Accessed 22 August 2017.
11. Lakshmi, S. and Sundareshwaran, P. (2019) An Android based Image Processing Application to Detect Plant Disease. International Research Journal of Engineering and Technology (IRJET), 6(5).
12. Petrellis, N. (2017) A Windows Phone Application for Plant Disease Diagnosis. Proc. of the 8th HAICTA, Chania, Greece.
13. Petrellis, N. (2019) Plant Disease Diagnosis with Color Normalization. Proc. of the IEEE MOCAST 2019, Thessaloniki, Greece